Nano-Structures & Nano-Objects 11 (2017) 7–12

Contents lists available at ScienceDirect

Nano-Structures & Nano-Objects

journal homepage: www.elsevier.com/locate/nanoso

Synthesis of GDC electrolyte material for IT-SOFCs using glucose & fructose and its characterization

Srikar Medisetti [a,1,2], Junsung Ahn [b,1], Sunaina Patil [a], Apoorva Goel [a], Yaswanth Bangaru [a], Gautam V. Sabhahit [a], G. Uday Baskar Babu [c], Jong-Ho Lee [b,*], Hari Prasad Dasari [a,*]

[a] Chemical Engineering Department, National Institute of Technology Karnataka, Mangalore-575025, India
[b] High-Temperature Energy Materials Research Center, Korea Institute of Science and Technology, Hwarangno 14-gil 5, Seongbuk-gu, Seoul 136-791, South Korea
[c] Chemical Engineering Department, National Institute of Technology, Warangal-506004, India

HIGHLIGHTS

- GDC synthesis using Glucose and Fructose organic additives.
- XRD and Raman confirm cubic fluorite structure.
- Dilatometer study reveal two shrinkage maxima (45 °C & 1450 °C).
- Ionic Conductivity at 700 °C in air is 1.13E−02 S cm^{-1}.

GRAPHICAL ABSTRACT

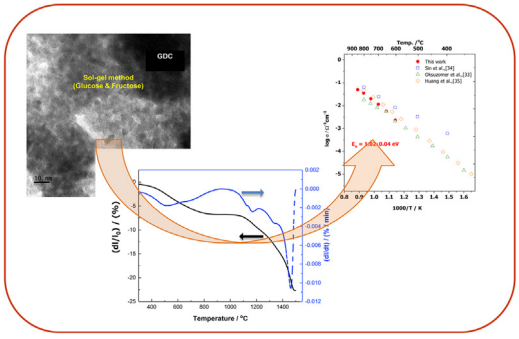

ARTICLE INFO

Article history:
Received 2 November 2016
Received in revised form 15 April 2017
Accepted 21 May 2017

Keywords:
Ceria
Electrolyte
IT-SOFCs
Dilatometer
Ionic conductivity

ABSTRACT

Nano-powder of gadolinium-doped-ceria (GDC, $Ce_{0.9}Gd_{0.1}O_2$) has been synthesized using a novel sol–gel method with glucose and fructose as organic additives. The main objective of the present study is to find the suitability of this synthesis method in synthesizing ceria-based SOFC electrolyte materials and evaluate its performance. The average crystallite/particle size obtained from XRD, TEM, BET surface area was found to be 4–12 nm. The phase was found to be cubic fluorite from XRD and further the structure and the nature of oxygen vacancies was confirmed using Raman spectroscopy. Dilatometer studies illustrated two shrinkage maxima (450 °C and 1450 °C). The ionic conductivity measurements were done using DC four-probe method on the GDC electrolyte sintered at 1500 °C. The sintered sample showed an ionic conductivity of 1.13E−02 Scm^{-1} at a temperature of 700 °C in the air, and the activation energy is 1.02 eV. The present study reveals that this synthesis method can be adaptable for synthesizing SOFC electrolyte materials.

1. Introduction

The ability of solid-oxide fuel cells (SOFCs) to operate on a variety of fuels makes it more economical than other fuel cells in small-scale, stand-alone and remote applications. Doped CeO_2 is increasingly replacing yttrium-stabilized-zirconia (YSZ) that was the traditional electrolyte for SOFCs at high operating temperatures due to its higher oxygen ionic conductivity at intermediate/low

* Corresponding authors.
E-mail addresses: jongho@kist.re.kr (J.-H. Lee), energyhari@nitk.edu.in (H.P. Dasari).

1 Equal contribution by the authors.

2 Present address: Otto H York Department of Chemical Engineering, New Jersey Institute of Technology, NJ 07102, USA.

http://dx.doi.org/10.1016/j.nanoso.2017.05.009
2352-507X/

operating temperatures of SOFCs [1]. Gd^{3+} and Sm^{3+} doped ceria shows higher ionic conductivity because of a smaller enthalpy associated between the doped cation (Gd^{3+} and Sm^{3+}) and the oxygen vacancy of the host lattice (ceria) [2,3]. This property is because of the close but slightly higher ionic radius of Sm^{3+} and Gd^{3+} compared to Ce^{4+} [4]. Thus, these excess oxygen vacancies formed can lead to higher ionic conductivity than its counterpart (pure ceria) [5]. Gadolinium-doped-ceria (GDC) electrolyte is today regarded as one of the promising material for intermediate and low-temperature SOFCs. Because an SOFC electrolyte needs to have near full density, nano-sized GDC powders are more desirable for their use compared to bulk powders. The higher specific surface area of nano-sized particles leads to faster densification and lower sintering temperature. Also their higher homogeneity results in better properties of the sintered materials [6].

A variety of methods can synthesize GDC material. These include hydrothermal [7,8], precipitation [9], decomposition, combustion, thermal evaporation [10], and reverse micelle [11]. In general, powder characteristics, and thus their synthesis route, significantly affect the densification kinetics and overall sinterability of the powder. In the past, many techniques like sol–gel thermolysis [12], cation-complexation [13] and glycine-nitrate process [14] have been used to achieve smaller GDC particle sizes between 9 and 17 nm and sintering temperatures between 1200 and 1500 °C. Prasad et al., has used co-precipitation method [15] and glycine-nitrate-process method [16] to bring down sintering temperatures. Apart from these synthesis methods, GDC material is also synthesized by EDTA-Citrate complexation process [17,18], microemulsion [19], and acryl amide polymerization [20] methods. In general, the powders prepared by these wet chemical methods is of high purity, homogeneity and depending on the nature of particle and agglomerate sizes the sintering temperature and time can be reduced when compared to GDC material prepared by solid-state reaction which requires high sintering temperature and time.

Suciu et al. [21,22] used the sol–gel method and organic additives—sucrose and pectin in acidic ambient to synthesize YSZ nanoparticles. In acidic conditions, hydrolysis of sucrose takes place resulting in glucose and fructose where glucose oxidizes to gluconic acid which acts as chelation agent and forms a complex with the metal. Sucrose and pectin are very high molecular weight compounds. They also form a cross-linkage pattern. So, to remove these organic compounds at a later stage heat treatment at higher temperatures would be needed. Heshmatpour et al. [23] modified this method and in basic pH, glucose and fructose were used as organic additives. The present study aims to synthesize SOFC electrolyte material (GDC) using this simple organic additives (glucose and fructose) and determine its sintering and ionic conductivity behaviors. The advantage of such kind of a synthesis method is that the addition of glucose and fructose can act as an efficient capping agent and helps in attaining more uniform particle size and apart from that these additives are relatively cheap, non-toxic, water soluble and easy to store at low temperatures. Besides, this synthesis method is environmentally friendly and takes only 24–30 h in total for the preparation are the two additional advantages. To the best of our knowledge, no reports are available on GDC material synthesized by this method using glucose and fructose additives. The present paper may give a real insight into this synthesis method in the development of SOFC materials and its impact on the performance.

2. Experimental

2.1. Sol–gel process using glucose and fructose

The sol–gel process is employed to obtain GDC nano-powder using D-glucose (Finar Chemicals) and D-fructose (Finar Chemicals) as organic additives. Stoichiometric amounts of $Ce(NO_3)_3{\cdot}6H_2O$ (SRL Chemicals) (55.54 g, 0.1280 moles) and $Gd(NO_3)_3{\cdot}6H_2O$ (CDH chemicals) (6.44 g, 0.0144 moles) are dissolved in distilled water (500 ml) and stirred to obtain a homogeneous solution. To the above solution, ammonium hydroxide (NH_4OH) (Spectrum reagents) was added drop by drop to achieve the pH around 9–10. Under vigorous stirring, with a weight ratio of 1:1, a mixture of D-glucose (51.28 g, 0.2847 moles) and D-fructose (51.28 g, 0.2847 moles) was added, and their mole ratio with metal ions is 2:1. The homogeneous solution is kept for stirring at room temperature for 2 h. The obtained solution is heated (100 °C/14 h) under constant stirring. A thick gel is obtained and transferred to a hot-air oven (120 °C/24 h). Polymerization (black powder) of the gel occurs during this step. Further, the black powder is heat treated at 350 °C/24 h to obtain nanocrystalline GDC powder (25 g).

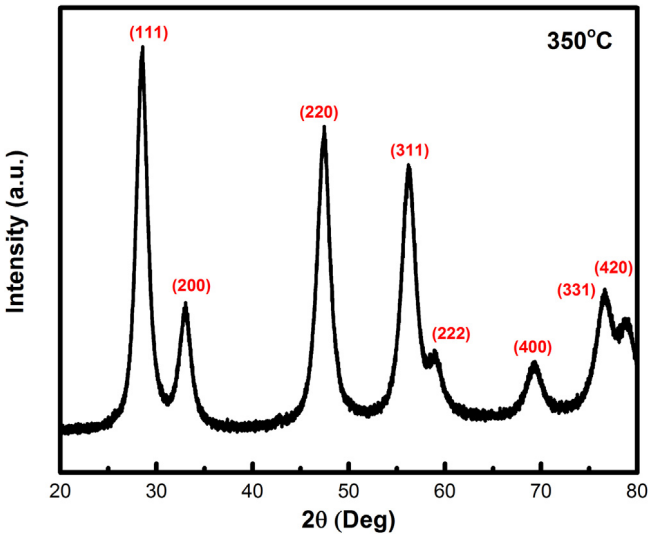

Fig. 1. XRD patterns of the calcined GDC powder.

2.2. Characterization techniques

The synthesized GDC nano-powder was characterized using different characterization techniques. XPERT-PRO diffractometer with Cu Kα radiation ($\lambda = 1.540498$ Å) is used to determine the phase of the nano-powder. The average crystallite size (d) in nm can be calculated with Scherrer equation given by

$$d = (0.9\lambda)/(\beta \cos\theta)$$

where, λ is the wavelength of the X-ray and β is the full width of the peak at half its maximum height at the respective 2θ values. To further confirm the phase of the powder, it is analyzed by Raman spectroscopy using BRUKER: RFS 27 with a laser intensity of 100 mW. A FE-SEM/EDS (field emission scanning electron microscope/energy dispersive spectroscopy) (Carl Zeiss Sigma/Oxford Instruments), was used to study the morphology and elemental analysis (Ce and Gd) of the sample. The surface area was measured using SMARTSORB—92/93 surface area analyzer. To view the particle size nature JEM 2100, JEOL TEM (transmission electron microscope) was used. The dilatometry studies were performed using Netzsch Dil 402C/3/G over a temperature range of 50 °C–1500 °C with a heating rate of 3 °C/min and the flow rate of air was maintained at 50 ml/min. The ionic conductivity of the sample was measured in the range of 850 °C to 600 °C by DC four-probe method using the precision current source (Keithley 6220, USA) and the multimeter (Keithley 2000, USA).

Table 1
Comparison of properties of GDC nano-powders prepared by various synthesis methods.

Synthesis method	Crystallite size (nm)	BET surface area (m^2/g)	Surface area equivalent particle size (nm)	Reference
Co-precipitation	8.7	68	12.2	[15]
Glycine nitrate process	17.0	42	18.4	[16]
Sol–gel thermolysis	10.0	64	13.1	[12]
Sol–gel (glucose and fructose)	4.7	71	11.7	[This study]

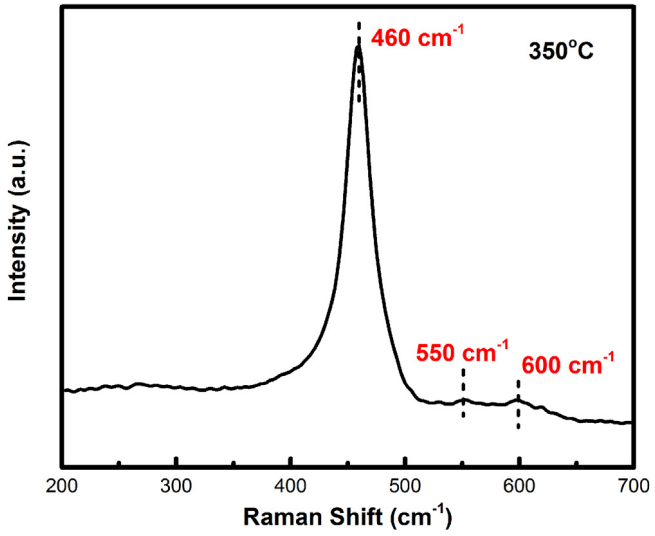

Fig. 2. Raman spectrum of the calcined GDC powder.

3. Results and Discussion

Fig. 1 depicts the XRD patterns of the GDC powder obtained upon calcination at 350 °C for 24 h. These peaks represent the presence of a phase and the crystallite size is nanocrystalline in nature. All the peaks obtained correspond to the cubic fluorite structure of ceria [12,24–28]. The peaks related to gadolinium oxide (Gd_2O_3) were not noticed, and this confirms that it is entirely doped into the ceria lattice [12,25]. The average crystallite size was calculated from XRD using the Scherrer equation and was found to be ∼4.7 nm. The lattice constant was found out to be ∼5.411 Å. Table 1 shows the crystallite size, BET surface area and its equivalent particle size of GDC nano-powder synthesized by various methods [12,15,16]. When compared to the other synthesis methods like co-precipitation method [15], glycine-nitrate process [16] and sol–gel thermolysis process [12] (Table 1), GDC nano-powder prepared by sol–gel method (using glucose and fructose) resulted in smaller crystallite size (∼4.7 nm) and particle size (∼11.7 nm) along with higher BET surface area (∼71 m^2/g).

From Fig. 2, a sharp and distinct peak can be seen at 467 cm^{-1}, which corresponds to the F_{2g} mode of Raman for cubic fluorite structured oxides [29]. As stated in literature, a vibrational mode at 360 cm^{-1} corresponds to the cubic phase of Gd_2O_3. The absence of this mode in the present spectra confirms that the Gd^{3+} ions occupied the interstitial spaces in the ceria lattice, and assures a solid-solution formation [14,30]. Nakajima et al. [31] stated that the vibrational modes associated with the wave number around

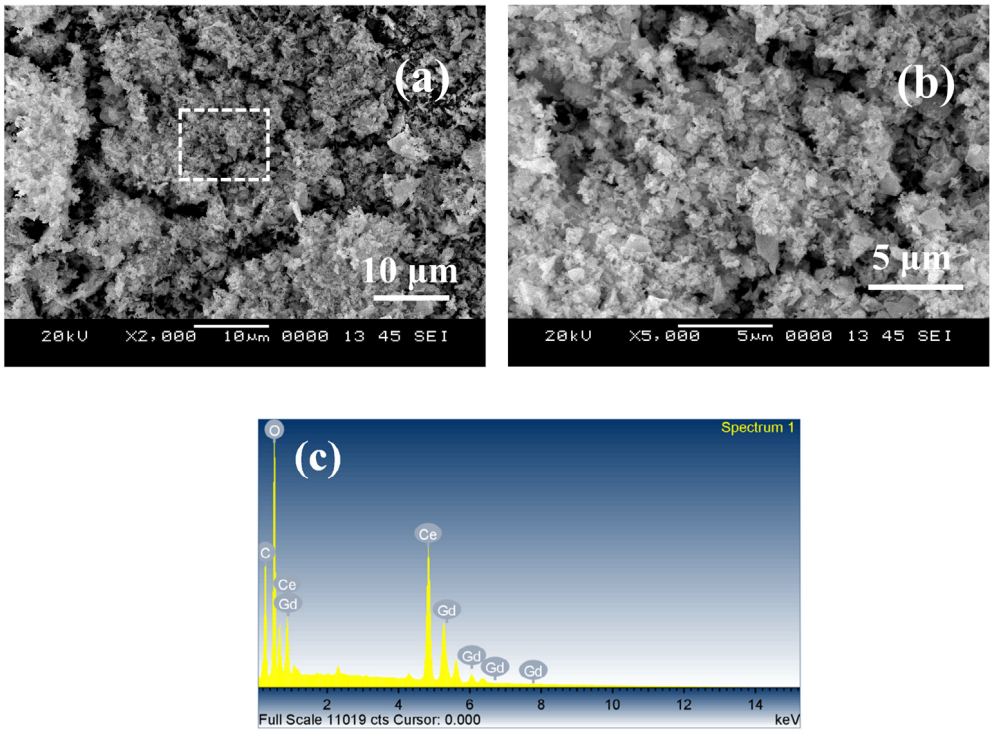

Fig. 3. (a) and (b) SEM micrographs of the calcined GDC powder and (c) EDS analysis obtained from Fig. 3(a).

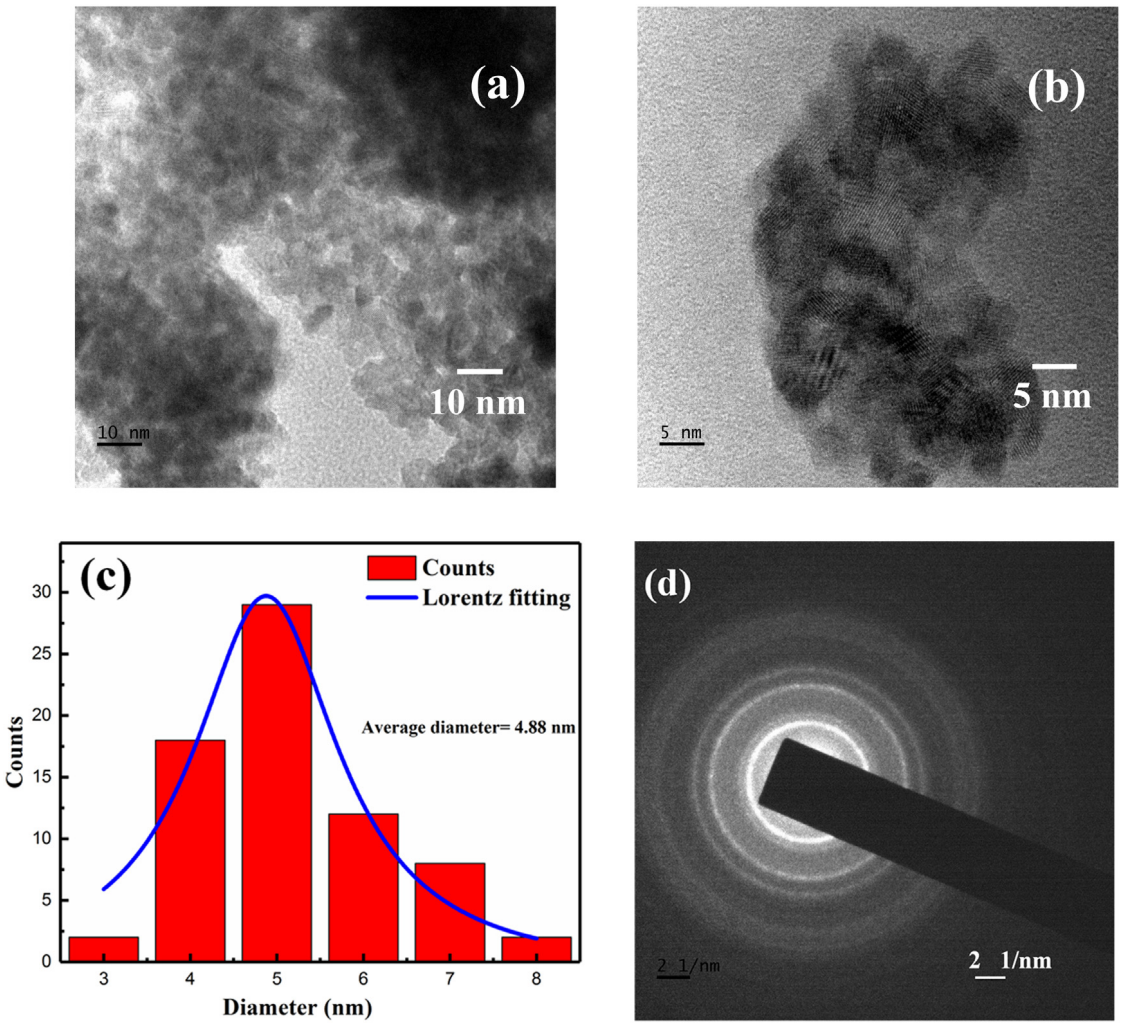

Fig. 4. (a) and (b) TEM micrographs of the calcined GDC powder, (c) TEM based particle size histogram (from Fig. 4(a)) and (d) SAED pattern of the obtained GDC powder.

Table 2
Composition of GDC nano-powder analyzed by energy dispersive spectroscopy.

Element	Wt%	Mole	Mole%
Ce	89	0.6343	90
Gd	11	0.0707	10

600 cm^{-1} are related to the defects in and around the intrinsic oxygen vacancies and the vibrational state near 550 cm^{-1} is created due to the extrinsic vacancies.

The synthesized GDC nano-powder calcined at 350 °C/24 h was analyzed using SEM to observe the morphological features present in the microstructure of the sample. As illustrated in Fig. 3(a) and Fig. 3(b), it can be observed that there is an agglomeration of the particles to a certain extent and the particles appear to be flaky in nature [32]. Table 2 displays the EDS analysis of the sample and shows that Ce and Gd has 89.96 and 10.03 mole%, respectively and confirms the GDC composition ($Ce_{0.9}Gd_{0.1}$). Fig. 4(a) and (b) shows the TEM images of the GDC powder, and it has the nanoparticle nature. From TEM images it can be observed that the nanoparticles are agglomerated. The quantitative measurement of the nanoparticle size is done by plotting the histogram from Fig. 4(a), fitted by Lorentz function is depicted in Fig. 4(c). The average nanoparticle size from the histogram is measured to be ~4.9 nm. The nanoparticle size obtained from TEM images was slightly greater than the average crystallite size obtained from XRD analysis. To further confirm the crystallinity of the obtained GDC nano-powder, selected-area electron diffraction (SAED) is carried out and the SAED image is shown in Fig. 4(d). The figure shows series of rings which define the polycrystalline nature of GDC nano-powder. From Fig. 4(d), it can be clearly observed that four most significant diffraction planes [(111), (200), (220) and (311)] that correspond to the cubic fluorite structure GDC sample and this further confirms the results obtained from XRD analysis.

Dilatometry studies for the synthesized sample were carried out till a temperature of 1500 °C. Fig. 5 depicts the shrinkage rate spectrum and the linear shrinkage curve. The GDC sample undergoes the sintering process with two shrinkage maxima. The maxima at 450 °C indicate the start of the sintering of the nanoparticles. The maxima at around 1450 °C indicate the presence of some hard agglomerates in the sample because of which the powder might have retained is original shape during densification. From the linear shrinkage curve in Fig. 5, it can be observed that the sample reaches a full shrinkage of about 23% at 1500 °C. The samples were heat treated at 1500 °C to attain full density to measure the ionic conductivity. From XRD (crystallite size, ~4.7 nm), TEM (particle size, ~4.9 nm), BET surface area (~71 m^2/g) and dilatometry studies, one can also observe that the synthesis method used in the present study resulted in high the surface area along with some hard agglomerates, and to decrease these hard agglomerates one has to optimize the glucose, fructose and metal nitrate mole ratios.

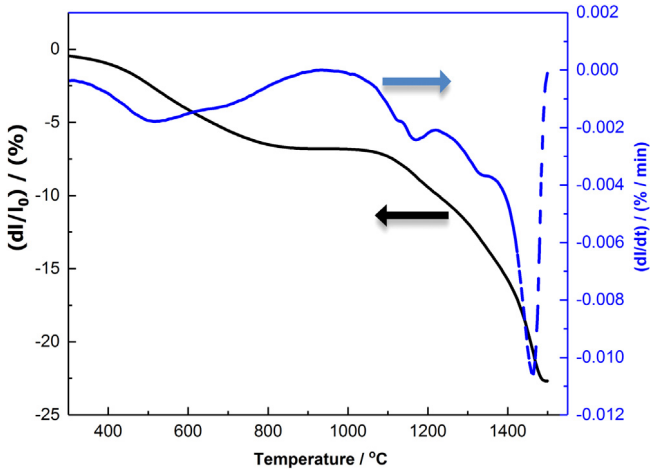

Fig. 5. Linear shrinkage and shrinkage rate curves of GDC green pellet from 50 °C to 1500 °C. (For interpretation of the references to color in this figure legend, the reader is referred to the web version of this article.)

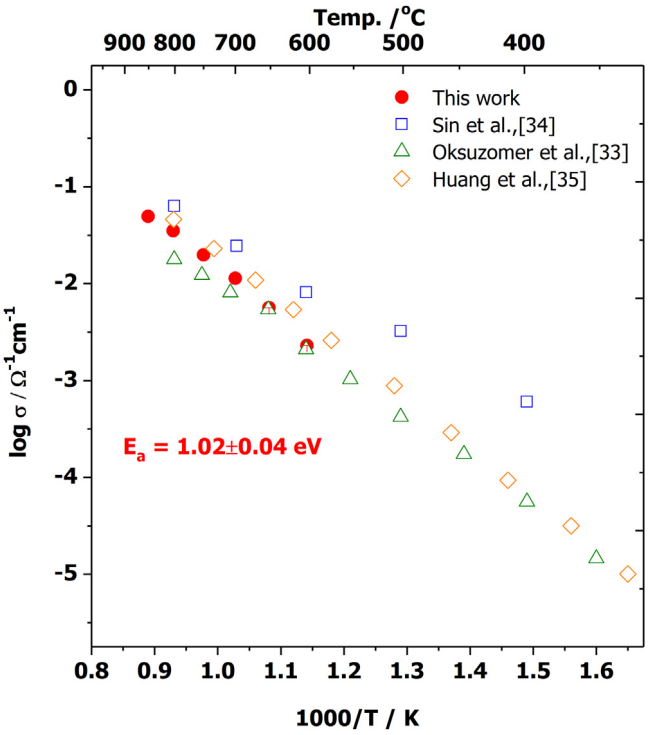

Fig. 6. Ionic conductivity data (from 600 to 850 °C) of GDC pellet sintered at 1500 °C/5 h.

Fig. 6 shows the Arrhenius plot of the GDC sample sintered at 1500 °C/5 h. The ionic conductivity measurements were carried from 600 to 850 °C in the air atmosphere. The conductivity data well matches within the range when compared to literature data [33–35]. The ionic conductivity obtained in the air is 1.13E−02 S cm^{-1} at a temperature of 700 °C, and the activation energy is 1.02 eV. The activation energy achieved in the present study is in the similar range obtained by Kuharuangrong [36] for the same amount of Gd-doped ceria electrolyte. The reason for such a high activation energy is may be due to additional grain boundary resistance and literature reports similar behavior with doped (Sm, Y) ceria materials [37,38]. Even though the reason is not entirely understood, segregation of different elements at grain boundaries, segregation of impurities and grain boundaries structural disorder may result in high grain boundary resistance for the ceria based electrolytes which are heat treated at critical sintering temperature [39–43]. The total conductivity in polycrystalline electrolyte materials under given temperature and surrounding atmosphere can be enhanced by following suitable modifications in composition, microstructure and processing. The properties of the grains and grain boundaries can be effected by composition, dopant concentration and processing conditions [44]. Kulkarni et al. [45], and Sui et al. [46], reported a conductivity of 0.97E−02 S cm^{-1} and 1.40E−02 S cm^{-1} at 700 °C, respectively, which is in agreement with the conductivity observed in the present study. Based on the conductivity results that were obtained in the range of 600–850 °C, GDC prepared by sol–gel method using organic additives (glucose and fructose) may be used as potential electrolyte material for SOFC applications. The topic for the forthcoming paper would be how to enhance the sinterability and ionic conductivity of GDC electrolyte material by controlling the powder characteristics through optimization of powder synthesis method.

4. Conclusions

GDC nano-powder have been successfully synthesized using a novel sol–gel method with glucose and fructose as organic additives. XRD and Raman spectroscopy results confirmed that the GDC nano-powder has cubic fluorite structure. FE-SEM and EDS analysis confirmed the agglomerate nature and elemental analysis (Ce, Gd) of GDC nano-powder. TEM analysis and particle size dispersion histogram of GDC nano-powder has a particle diameter of ∼4.9 nm. Dilatometer studies revealed two peaks (450 °C and 1450 °C) of shrinkage behavior indicating that the GDC nano-powder synthesized in this work is the combination of nano-particles and hard agglomerates. From the dilatometry studies the sintering temperature is fixed at 1500 °C and the ionic conductivity of the obtained GDC electrolyte is 1.13E−02 S cm^{-1} with an activation energy of 1.02 eV. The synthesis method used in this paper can give a new scope for the development of SOFC materials.

Acknowledgments

This work was supported by KIST-IRDA alumni Project (Grant No. 2Z04820-16-095) and KETEP (Grant No. 20143030031430). SM, AG, YB and GVS would like to thank chemical engineering department, NITK for carrying out their B.Tech final year project under the guidance of HPD. We would like to thank DST and sophisticated analytical instrument facility (SAIF) at India Institute of Technology (IIT) Madras for providing Raman data of our samples using FT-Raman spectrometer (Bruker FRS) instrument.

References

[1] V.V.V. Kharton, F.M. Figueiredo, L. Navarro, E.N. Naumovich, A.V. Kovalevsky, A.A. Yaremchenko, et al., J. Mater. Res. 36 (2001) 1105.
[2] R. Gerhardt-Anderson, A. Nowick, Solid State Ion. 5 (1981) 547.
[3] J. Kilner, Solid State Ion. 8 (1983) 201.
[4] H.C. Jang, D.S. Jung, J.H. Kim, Y.C. Kang, Y.H. Cho, J.-H. Lee, Ceram. Int. 36 (2010) 465.
[5] S. Zha, C. Xia, G. Meng, J. Power Sources 115 (2003) 44.
[6] N.Q. Minh, J. Am. Ceram. Soc. 76 (1993) 563.
[7] J.-S. Lee, S.-C. Choi, Mater. Lett. 58 (2004) 390.
[8] N.-C. Wu, E.-W. Shi, Y.-Q. Zheng, W.-J. Li, J. Am. Ceram. Soc. 85 (2002) 2462.
[9] F. Zhang, J. Appl. Phys. 95 (2004) 4319.
[10] W.H. Lee, P. Shen, J. Solid State Chem. 166 (2002) 197.
[11] J. Zhang, X. Ju, Z.Y. Wu, T. Liu, T.D. Hu, Y.N. Xie, et al., Chem. Mater. 13 (2001) 4192.
[12] D.H. Prasad, J.-W. Son, B.-K. Kim, H.-W. Lee, J.-H. Lee, J. Eur. Ceram. Soc. 28 (2008) 3107.
[13] R.O. Fuentes, R.T. Baker, Int. J. Hydrog. Energy 33 (2008) 3480.

[14] L.D. Jadhav, M.G. Chourashiya, A.P. Jamale, A.U. Chavan, S.P. Patil, J. Alloys Compd. 506 (2010) 739.
[15] D. Hari Prasad, H.-R. Kim, J.-S. Park, J.-W. Son, B.-K. Kim, H.-W. Lee, et al., J. Alloys Compd. 495 (2010) 238.
[16] D. Hari Prasad, J.-W. Son, B.-K. Kim, H.-W. Lee, J.-H. Lee, J. Ceram. Proc. Res. 11 (2010) 176.
[17] S. Li, L. Ge, H. Gu, Y. Zheng, H. Chan, L. Guo, J. Alloys Compd. 509 (2011) 94–98.
[18] K.C. Anjaneya, M.P. Singh, J. Alloys Compd. 25 (2017) 871–876.
[19] J. Chandradass, B. Nam, K.H. Kim, Colloids Surf. A 348 (2009) 130–136.
[20] A. Tarancon, G. Dezanneau, J. Arbiol, F. Peiro, J.R. Morante, J. Power Sources 118 (2003) 256–264.
[21] C. Suciu, L. Gagea, A.C. Hoffmann, M. Mocean, Chem. Eng. Sci. 61 (2006) 7831.
[22] C. Suciu, A.C. Hoffmann, P. Kosinski, J. Mater. Process. Technol. 202 (2008) 316.
[23] F. Heshmatpour, R.B. Aghakhanpour, Powder Technol. 205 (2011) 193.
[24] A. Arabaı, M.F. Öksüzömer, Ceram. Int. 38 (2012) 6509.
[25] A.Z. Liu, J.X. Wang, C.R. He, H. Miao, Y. Zhang, W.G. Wang, Ceram. Int. 39 (2013) 6229.
[26] G. Accardo, C. Ferone, R. Cioffi, D. Frattini, L. Spiridigliozzi, G. Dell'Agli, J. Appl. Biomater. Funct. Mater. 14 (2016) 35.
[27] M.K. Rath, B.H. Choi, M.J. Ji, K.T. Lee, Ceram. Int. 40 (2014) 3295.
[28] M.K. Rath, M.-J. Lee, K.-T. Lee, Ceram. Int. 40 (2014) 1909.
[29] L.N. Gu, G.Y. Meng, Mater. Res. Bull. 43 (2008) 1555.
[30] A. Mineshige, Solid State Ion. 135 (2000) 481.
[31] A. Nakajima, A. Yoshihara, M. Ishigame, Phys. Rev. B 50 (1994) 13297.
[32] R.V. Mangalaraja, S. Ananthakumar, Kasimayan Uma, Romel M. Gimenez, et al., J. Ceram. Proc. Res. 13 (2012) 15.
[33] M.A.F. Öksüzömer, G. Dönmez, V. Sariboğa, T.G. Altinçekiç, Ceram. Int. 39 (2013) 7305.
[34] A. Sin, Y. Dubitsky, A. Zaopo, A.S. Aricò, L. Gullo, D. La Rosa, et al., Solid State Ion. 175 (2004) 361.
[35] K. Huang, M. Feng, J.B. Goodenough, J. Am. Ceram. Soc. 81 (1998) 357.
[36] S. Kuharuangrong, J. Power Sources 171 (2007) 506.
[37] D. Ding, B. Liu, M. Gong, X. Liu, C. Xia, Electrochim. Acta 55 (2010) 4529.
[38] C. Tian, S.-W. Chan, Solid State Ion. 134 (2000) 89.
[39] M.J. Verkerk, B. Middelhuis, A. Burggraaf, Solid State Ion. 6 (1982) 159.
[40] M.J. Verkerk, A.J.A. Winnubst, A.J. Burggraaf, J. Mater. Sci. 17 (1982) 3113.
[41] Z.-P. Li, T. Mori, G.J. Auchterlonie, J. Zou, J. Drennan, Appl. Phys. Lett. 98 (2011) 093104.
[42] D.W. Joh, M.K. Rath, J.W. Park, J.H. Park, K.H. Cho, S. Lee, et al., J. Alloys Compd. 682 (2016) 188.
[43] X. Guo, Solid State Ion. 81 (1995) 235.
[44] S. Hui, J. Roller, S. Yick, X. Zhang, C. Decès-Petit, Y. Xie, R. Maric, D. Ghosh, J. Power Sources 172 (2007) 493–502.
[45] S. Kulkarni, S. Duttagupta, G. Phatak, RSC Adv. 4 (2014) 46602–46612.
[46] A.Z. Liu, J.X. Wang, C.R. He, H. Miao, Y. Zhnag, W.G. Wang, Ceram. Int. 39 (2013) 6229–6235.